Bio-inspired laminate design exhibiting pseudo-ductile (graceful) failure during flexural loading

Authors: Robert Malkin, Mehdi Yasaee, Richard S. Trask, Ian P. Bond*

University of Bristol, Advanced Composites Centre for Innovation and Science,
Department of Aerospace Engineering, Queen's Building, University Walk, Bristol.
BS8 1TR. United Kingdom.

* Corresponding author Tel.: +44 (0) 117 33 15321

E-mail: i.p.bond@bristol.ac.uk

Abstract

Discontinuous reinforcement phases are often observed in high toughness natural materials, for example, nacre. The aim of this study is to introduce a degree of ‘pseudo-ductility’ to fibre reinforced polymer materials by exploiting such discontinuities. The work presented aims to take a simple concept of discrete material sections and apply it in the form of ply cuts in a carbon fibre reinforced polymer. A variety of specimen types which encompass the principles inspired by the architecture of nacre were tested in four point bend flexure and the failure processes investigated. Finite element analysis was also carried out to understand stress conditions around ply cuts and their role in the observed failure. It was observed that ply cut spacing and ply cut density were important parameters in achieving 'pseudo-ductile' failure.

Keywords:

A. Carbon fibre;

A. Laminates;

B. Damage tolerance;

B. Stress concentrations.

1 Introduction

1.1 Nacre

Nacre is a composite material found in the inner layers of mollusc exoskeleton and features a highly discontinuous structure. The main function of this exoskeleton is the protection of the inner soft tissue from external damage. Nacre is a hierarchical material and it's remarkable physical properties are the subject of ongoing debate [1–7]. The structure of nacre comprises lamellae of discontinuous platelets. The platelets are discrete hexagonal calcium carbonate (aragonite) tiles, embedded in a viscoelastic protein matrix arranged in a 'brick and mortar' microstructure, resulting in two levels of hierarchy [8], shown in Figure 1 (adapted from [9]). The tiles of aragonite are typically 300-500nm thick with the organic layer being 20-30nm in thickness. An interesting feature of nacre is the very high percentage of the mineral phase, with values of around 95% of the total weight. In nacre, the unique viscoplastic deformation of the organic interface and the crack delocalisation of the layered microstructure of the inorganic aragonite leads to an increase in fracture toughness; this is typically 20-30 times that of synthetic aragonite and fracture strength three orders of magnitude higher than monolithic calcium carbonate [10]. This remarkable toughness and strength, from a relatively simple arrangement of 'tiles' and 'glue', demonstrates the importance of structural design over base material properties. As observed by *Knipprath et. al.* [11], an exact representation of nacre, experimentally or with finite element analysis (FEA) is extremely challenging due to the multi-level hierarchy material intricacies and complex pseudo-ductile failure mechanisms at different length scales, such as interlayer deformation, crack deflection, microbuckling and delamination [12]. Direct mimicry of this system is currently beyond the scope of engineering composite materials but the synthesis of these ‘design rules’ to yield ‘graceful degradation’ within a brittle based system is possible and the motivation behind this study.

1.2 Fibre reinforced polymers

Unidirectional (UD) fibre reinforced polymers (FRP) are generally considered to be continuous in nature, with the reinforcing fibre tows essentially uninterrupted along the length of the laminate. There are exceptions to having a continuous fibre arrangement, which are a necessity of real component design and manufacture (Figure 2).

- Automatic lay up; during manufacture of large components, the spool of pre-impregnated tape will need periodic replacement resulting in a discontinuous ply region, often a butt joint. Figure 2a shows two ply terminations sandwiched between two continuous plies.
- Tapering; if a reduction in component thickness is required, this is achieved by a series of ply-drops. Figure 2b shows a single ply drop reducing the thickness of the laminate by one lamina.
- Embedment; occasionally features such as health monitoring devices (e.g. fibre optics or strain measurement), Figure 2c.

The work presented herein discusses research conducted into the effect of ply terminations on the fracture behaviour of laminated FRPs. By selectively introducing controlled discontinuities it has been shown that the catastrophic failure commonly observed in UD composites can be reduced by creating a number of sub-critical fractures sites distributed throughout the structure.

In contrast to continuous FRPs, discontinuous FRP systems in the form of sheet-moulding compounds (e.g. Hexcel HexMC) consist of short ‘chips’ of pre-preg cut to various sizes and oriented in various directions. The benefit of such a material architecture is an ability to mould very complex 3D components which would not be possible with continuous fibre systems. The nature of discontinuous fibre systems means that there are many ply terminations and resin rich areas. Work by *Feraboli et.al*. [13] identified resin rich areas as well as resin-starved areas to be causes of laminate failure. The work herein takes a fundamental approach to understanding ply discontinuities and their effect on fracture properties.

1.3 The influence of ply cuts on fracture behaviour

Within a laminate, resin rich areas are often avoided as they can act as crack initiation sites due to localised stress concentrations [9][10]. However, this property can be utilised to control the location of crack initiation as well as controlling the subsequent propagation. If a ply cut is introduced within a laminate there will be a resin pocket at the location of the cut, as seen in Figure 2. To the authors knowledge the effect of this resin pocket geometry/ply cut spacing on flexural fracture properties of a FRP laminate has not been investigated. By altering the width of separation between the two ply ends a simple way of understanding the resin pocket's influence on fracture behaviour can be studied. It is believed that these ply terminations essentially introduce a number of 'weak' links within the laminate. By correctly coordinating these 'weak' links it is possible to generate sequential or 'graceful' failure by replacing a single large catastrophic crack with a number of smaller sub-critical cracks.

Literature shows that cut plies can be used to understand tapering effects, therefore, the work presented may be applicable to tapered laminates as well as those with a uniform thickness [16]. The idea of a 'weak link', which essentially states that each ply cut acts independently unless the distance separating adjacent cuts is less than a critical value, has also been suggested [17–19]. *Richards et al*. [18] determined a loss in tensile strength of about 15% in CFRP irrespective of the number of ply cuts, given that the separation distance between ply cuts was above this critical value. The work of *Darby et al*. [17] would suggest that for IM7/8552 (the material used in this study) this length would be approximately 0.15mm. This criticality may, therefore, be exploited and allow for laminate designs capable of exhibiting progressive failure. An alternative study on the tensile fracture of a different material system by *Taketa et al.* [20] showed the benefits of including ply cuts distributed within pre-preg to permit complex part geometries to be compression-moulded. The authors also derive an accurate strength calculation for laminates containing ply cuts. It is apparent from these studies [15-18], that the control of a number of 'weak links' within a brittle material has the potential for graceful failure in engineering materials, as observed in the biological kingdom.

2 Specimen manufacture and test procedure

2.1 Specimen manufacture

All specimens were manufactured from UD IM7/8552 CFRP pre-impregnated carbon/epoxy tape (Hexcel Composites, UK) of nominal cured ply thickness 0.125mm and autoclave cured according to manufacturers guidelines. Ply lay up was carried out in a clean environment and plies debulked for 15 minutes every 4 plies to remove entrained air. Post cure, laminates were cut on a diamond wheel, ground to specified dimensions and then polished using 400/800/1200 grade SiC to minimise edge effects. For specimens which had embedded ply cuts, the ply termination spacing was a control variable and investigated for its influence on the failure process. Preliminary testing showed that hand lay-up was not refined enough to allow for precise control over the ply termination spacing. To overcome this problem, a vacuum assisted lay-up positioning guide was developed, show in Figure 3.

The guide allowed for precise alignment of the pre-preg prior to consolidation of stacked plies. Double plies were chosen over individual plies in all of the specimens to aid optical measurement of the crack propagation as well as allowing for more consistent alignment of individual cut plies. It is expected that all of the behaviour observed in this study will also apply to single thickness ply cuts.

2.2 Test procedure

All the specimens manufactured were tested under quasi-static flexure in four point bending. The testing procedure followed the ASTM standard D7264/D7264M [21]. For all the flexural experiments the major and minor spans were 150mm and 75mm, respectively. The mid-span deflection of the specimens was recorded via a linear potentiometric displacement transducer (LPDT) (Sakae 13FLP, 25mm range). All tests were performed at a cross-head displacement of 1mm/minute and performed on an Instron 3343 screw driven electromechanical test machine with a 1kN load cell. For each specimen design 8 replicates were tested.

2.3 Effect of ply cut on laminate

Microscopy of prototype laminates showed a significant deformation of fibres due to the void induced by a ply cut. This deformation of surrounding fibres arising from the autoclave manufacturing process for different ply cut spacings in each laminate prior to testing is shown in Figure 4.

With small ply spacings (<1mm) surrounding fibres were not observed to deform significantly (Figure 4a,b) and the resin pocket was able to maintain a rectilinear shape, although Figure 4b shows some lateral movement during autoclave cure. It is interesting to note that the corners of the resin pockets are very sharp and are expected to cause significant stress concentrations within the resin pocket. For larger spacings (Figure 4c,d) the ply spacings have become highly deformed and almost prismatic in shape. This warping is attributed to the lack of fibres in the space between the ply ends and resin flowing from the surrounding areas to fill the void. This warping will have a large effect on the local fibre fraction and be detrimental to properties such as compressive strength. Given this added complexity of geometry/material property change this study was limited to studying the more rectilinear resin pockets caused by ply cut spacings of 0.2, 1.0 and 2.0mm respectively.

3 Specimen design and testing

Five specimen designs, A-E, were manufactured and tested to evaluate flexural failure (see Figure 5). The design strategy was based on an iterative approach where desired failure processes observed in one design were incorporated into the next.

For all of the 5 designs the beam dimensions were identical, with the location and number of ply cuts varying between each. Figure 5 shows the beam dimensions as well as ply cut locations for each of the five designs. All specimens were 24 plies in thickness and had cured average thicknesses of 2.91mm. Specimens were 12.7mm in width and cut to 200mm in length. No ply cuts were positioned outside of the minor span and as such all ply cuts were located within the uniform bending moment of the four point bend test.

3.1 Testing and Observed Failure

3.1.1 Design A

Design:

Specimens comprised 24 UD plies with no ply terminations, shown in Figure 5A. These specimens served as a baseline and to observe flexural failure mechanisms in conventional UD laminates. Testing to failure was expected to be catastrophic.

Failure:

All specimens failed with a catastrophic load drop with the specimen either; fracturing on the tensile surface with a large irregular delamination around the neutral axis of the specimen, or, into 2-3 individual fragments by way of explosive fracture. The location of initial failure was difficult to establish in all specimens but appeared to originate near one of the minor span supports. The average strength (calculated at peak load) of the specimens, as calculated according to the ASTM standard, is shown in Table **1**. A representative load displacement curve is shown in Figure 6.

3.1.2 Design B

Design:

From preliminary prototype testing it was found that specimens with ply cuts showed a significant sensitivity to the ply cut spacing. Design B allowed a simple scenario whereby the effect of ply cut spacing could be investigated. Laminates were manufactured with a single ply cut on the tensile surface, as shown in Figure 5B. Specimens were loaded until a significant delamination (length>40mm) had developed on the tensile surface. Ply spacings of 0.2, 1.0 and 2.0mm were tested, with 0.2mm being the limit of ply end separation achievable during manufacture.

Failure:

During loading two distinct failure events occurred, a resin pocket failure and a subsequent delamination. The resin pocket failure was identified by a small (<1N) load drop as well as a concurrent audible 'snap', in agreement with the findings of *Cui et al.* [22]. The loads at which both events occurred as well as the strength (calculated at the deflection at which delamination occurred) are shown in Table **2**. The delamination loads are consistent between all three ply cut spacings, as would be expected given that delamination load is governed by the critical strain energy release rate, *Gc*. The significant difference in resin pocket failure for each ply cut spacing is investigated with finite element analysis (FEA) in a section 4. A representative load displacement curve is shown in Figure 6.

3.1.3 Design C

Design:

As a first attempt to introduce a number of 'weak links' into a laminate, Design C was conceived. The design, shown in Figure 5C, has 4 ply cuts in a design similar to that seen in nacre. This specific design hoped to achieve pseudo-ductile failure as it was expected that the failure would initiate on the tensile surface and propagate steadily from one cut to the next. Spacings of 0.2, 1.0 and 2.0mm were tested until the top resin pocket (closest to the neutral axis) was visually observed to be the source of delamination. It was expected that failure would occur sequentially, as illustrated in Figure 7. Failure was expected to progress in the following order; (i) linear elastic response of the beam, (ii) fracture of the resin pocket nearest the tensile surface (greatest in-plane strain), (iii) delamination initiates at top of resin pocket, (iv) resin pocket failure at one of the two resin pockets on delamination interface, (v) delamination from second resin pocket to final resin pocket, (vi) resin pocket failure and (vii) final delamination failure. Upon reaching point (vii), the test was terminated. The remaining 18 continuous plies were assumed to be undamaged other than minor surface damage caused by delamination.

Failure:

A 1.0mm prototype specimen at the point considered final failure is shown in Figure 8. Specimens with a ply termination spacing of 0.2mm were observed to fail very differently to larger spacing specimens. The 0.2mm spacing samples all failed with a single load drop. There were no progressive or individual failures at the ply cuts. Of the 8 samples tested all 8 failed with a single load drop. The 1.0 and 2.0mm spacing samples however all showed a level of progressive failure with 2-4 small individual load drops. Of the 1.0mm spacings all 8 samples exhibited more than 2 individual load drops, while 6 of 8 samples of the 2.0mm spacing samples exhibiting more than 2 individual load drops. This variation in consistency is believed to be due to the complex morphology of resin pockets with ply spacings >1.0mm. There is a clear separation of failure process between the two ply cut spacing groups, smaller (0.2mm) and larger (>1.0mm). Figure 9 shows representative load displacement curves for all three tested ply cut spacings and strengths (calculated at the point of first visible delamination) are given in Table **1**.

3.1.4 Design D

Design:

Based on the multiple load drops observed in the failure of design C and knowing the importance of ply cut spacing it was hoped that a simple scaling of the design would allow for a large number of distinct load drops without catastrophic failure. Laminates were manufactured with 18 ply termination regions with the central portion of the beam shown in Figure 5D. The specimen design is effectively three lower sections of flexural type C specimens stacked together. Following results obtained from flexural type C specimens, three ply spacing values were chosen; 0.2, 1.0 and 2.0mm, with the hope of achieving stepped failure throughout the sample.

Failure:

Contrary to the expected failure process all samples, of all ply separations, failed without individual load drops or identifiable delaminations. All of the samples failed with a single large load drop resulting in a complex delamination pattern. Out of the 8 replicates, 3 showed delaminations on the compressive surface, 3 on the tensile surface and 2 on both. This suggests both compressive and tensile failures within the laminate. While untested, we hypothesise the mixed failure modes to be indicative of interaction between individual resin pockets. The alignment and number of ply terminations in a relatively small volume of material may give rise to complex stress field interactions. The strengths of design D specimens are given in Table 1 and a representative load displacement curve is shown in Figure 6.

3.1.5 Design E

Design:

Combining principles learnt from previous designs and considering the possible ply cut interactions, a final design process was undertaken.

-Design B showed that the ply cut spacing was an important factor in determining the failure load of the resin or resin/ply interface.

-Design C showed that sequential failure in flexure could be achieved to some extent. It also indicated that a ply cut spacing of 0.2mm did not fail progressively, while 1.0mm was more consistent in providing a stepwise failure than a 2.0mm spacing.

-Design D showed that simply scaling the effect observed in design C does not allow for multiple sub-critical failures. While the exact failure of design D remains unclear, it is felt likely that the number of ply cuts was too high for the volume of space which they occupied and/or the ply cuts were too close to one another thereby creating an interference effect. This interference may result in the magnification of stress found within a single ply spacing. Thus, Design E was based upon; (a) a ply cut spacing of 1.0mm, (b) ply cuts would be located in such a way as to avoid bunching or unnecessarily close proximity between ply cuts, (c) a nacre inspired arrangement of ply cuts. The designed laminate is shown in Figure 5E.

Failure:

Samples were loaded until only the continuous plies on the compressive surface remained un-fractured. The average strength of the design is given in Table **1**. Failure of all 8 specimens was progressive and did not exhibit any large load drops. The specimens all failed with between 5 and 8 individual small load drops, as indicated in Figure 10 and a prototype sample shown at various stages of failure in Figure 11.

4 Finite Element Analysis

In order to help explain the difference between failures observed for samples with different resin pocket spacings, especially design B, simple linear elastic FEA was undertaken (Comsol 4.3a). The aim of the FEA was to understand the nature of internal stresses around the ply cuts at a single resin pocket prior to any failure. The test procedure of design B (1 single resin pocket on the tensile surface of the beam) was replicated for this FEA study, at a number of ply cut spacings.

4.1 Model details

The models were static 2D linear orthotropic elastic with geometric non-linearity activated. The elements were six noded plane-strain quadratic free triangular type. The laminate was modelled as an orthotropic solid, the resin pocket and rollers as isotropic solids, with material properties given in Table **3**. The model replicated the loading conditions of the real beam as shown in Figure 12. In order to maintain an equal mesh density for each of the three resin pockets, the resin pocket area was contained within a rectangular section of 8mm width and 0.5mm height, which is simply a way of ensuring consistent element size (and density) which may be affected by the meshing algorithm, this section is shown in Figure 12. The rollers were modelled as mild-steel with contact conditions between the roller-composite surfaces. The lower rollers were fixed with the upper rollers given a negative vertical displacement of 2mm which is a displacement well below the displacement at which failure occurred in real samples. It is important to remember that actual stress values at corners predicted by FEA are highly dependant upon the mesh density [23]. As there is a relatively sharp resin pocket corners in the model, peak stresses will occur at the corners and will increase with increasing mesh density. The numerical singularities found at the corners of the resin pocket were avoided by taking an offset enquiry line 25µm away from the resin composite boundary, a technique used by other authors [23], as shown in Figure 12.

A mesh sensitivity study was undertaken to ensure that peak stresses were independent of element size and were based on a ply cut spacing of 1mm, the results of which are included in the appendix. The complete model comprised of 112k elements.

4.2 Results

σ_{11}, σ_{12} and σ_{22} stresses were probed at the top and at the side of the resin pocket (as illustrated with the red and blue lines in Figure 12, respectively). The σ_{11} stresses at the top of the resin pocket (both above and below the top of the resin pocket) were on average an order of magnitude higher than the σ_{12} and σ_{22}, and were thus chosen as the stresses to be reported and discussed. The stress values for different ply cut spacings are shown in Figure 13 and Figure 14. Figure 13 clearly shows a strong relationship between the stress intensity as well as the stress distribution above the resin pocket. The σ_{11} values below the top of the resin pocket do not show such a significant dependence on the ply cut spacing. The σ_{11} stress distributions for each of the tested spacings are shown in Figure 15.

An interesting feature arises from the stress distributions shown in Figure 13 and visually in Figure 15. The 1.0, 2.0 and 4.0mm spacings have two separated peaks while the 0.2 and 0.5mm appears to have a single peak. It should be noted that given the element size of approximately 3μm in and around the resin pocket, 167 and 67 elements represent the width of the resin pocket for 0.5 and 0.2mm spacings respectively. Given this fine mesh around the resin pocket it would be expected that a double peak, if present, would be observed. A further mesh refinement was carried out with 4 times the number of elements spanning the resin pocket and no double peak was identified. The lack of the double peak suggests that the high stress regions found at the corners of the 0.2 and 0.5mm resin pockets have superimposed to form a single high stress region, with the average stresses between the stress peaks being higher than the larger resin pockets. Therefore, it can be hypothesised that a reduction in ply cut spacing increases not only the peak stress but also the average stress around the resin pockets. This suggests that the reason for the lower resin pocket failure loads for design B is due to the stress state around the smaller resin pocket reaching its failure stress at a lower displacement.

5 Discussion

Experimental work was aimed at improving upon the catastrophic failure observed in UD design A specimens. This has been achieved by allowing for multi-stage fracture which comes at a sacrifice in ultimate flexural strength, as indicated in Table 1. Fracture of design B laminates showed that the ply cut spacing had a significant effect on resin pocket geometry and flexural failure. The suggestion as to the origin of this effect is explained by the FEA analysis where it is shown that the peak stress and average stress is proportional to the ply cut spacing, with smaller spacings resulting in higher stresses. This suggests that the reason for the difference in failure load for design B, Table 2, is due to a geometric effect of the resin pockets on the surrounding stress field. In effect the smaller resin pockets do not need to experience as much strain to fail due to their geometrical susceptibility to higher stress states.

Design C further explored the effect of ply cut spacing and the subsequent fracture process. The design also showed a highly significant effect of ply cut spacing on observed failure, as expected from the FEA analysis. The embedded resin pockets can be seen to act as crack stoppers which prevent delamination. Therefore, for small spacings the delamination which originates on the tensile surface is free to delaminate through the specimen without constraint. However, for larger ply spacings the delaminations will encounter resin pockets which will inhibit the delamination until the resin pocket itself fails allowing the delamination to continue.

The failure of design D suggests that a simple scaling of design C does not work. The exact reason for the interlaminar failure is unknown, the authors suggest that it may be due to alignment and/or ply cuts interacting within the localised volume which they occupy.

Design E achieved a progressive failure characterised by a number of small load drops, very different to the failure observed in design A, as shown in Figure 10. However, there is a consequent reduction in global flexural strength caused by the inclusion of ply cuts.

6 Conclusion

It has been shown that the catastrophic flexural failure observed in monolithic UD laminates can be mitigated by the judicious introduction of ply cuts within the laminate. By coordinating the location of ply cuts and taking ply cut separation into account a single large catastrophic fracture can be replaced with a number of smaller fractures. The reduction in flexural strength suggests that the utilisation of such a design strategy would need to be suited to an environment where pseudo-ductile fracture is a greater necessity than ultimate strength or situations where resin pockets are an inevitable outcome of the layup design e.g. ply drops. The FEA work conducted also suggests ply cut spacing to have a very significant effect on the stress field around the resulting resin pocket. This result is expected to be of significant importance in the design for manufacture via automatic tape lay-up machines.

7 Acknowledgements

The authors kindly acknowledge; Rolls Royce Plc. and Great Western Research for funding the research, Ian Chorley and Simon Chilton for help with sample preparation, Julie Etches for assistance with mechanical testing.

8 Appendix

Using the stress enquiry line 25μm above the top of the resin pocket and probing the peak stresses, the element size at which convergence occurred corresponded to an element size of 8.3μm within the resin pocket region, as shown in Figure 16.

This gives 80 elements in the thickness (250μm) of the resin pocket.

9 References

[1] R. Rabiei, S. Bekah, and F. Barthelat, "Failure mode transition in nacre and bone-like materials.," *Acta biomaterialia*, vol. 6, no. 10, pp. 4081–9, Oct. 2010.

[2] A. P. Jackson, J. F. V Vincent, and R. M. Turner, "The mechanical design of nacre," *Proc. R. Soc. Lond. B*, vol. 234, pp. 415–440, 1988.

[3] K. S. Katti, D. R. Katti, S. M. Pradham, and A. Bhosle, "Platelet interlocks are the key to toughness and strength of nacre," *Journal of Material Research*, vol. 20, no. 5, pp. 1097–1100, 2005.

[4] B. J. Gruner and G. Mayer, "Measuring Works of Fracture in Nacre-Inspired Ceramic Composite Beams." Univeristy of Washington, MSc Thesis, p. 29, 2006.

[5] K. Bertoldi, D. Bigoni, and W. J. Drugan, "Nacre: An orthotropic and bimodular elastic material," *Composites Science and Technology*, vol. 68, no. 6, pp. 1363–1375, 2008.

[6] F. Barthelat, H. Tang, P. Zavattieri, C. Li, and H. Espinosa, "On the mechanics of mother-of-pearl: A key feature in the material hierarchical structure," *Journal of the Mechanics and Physics of Solids*, vol. 55, no. 2, pp. 306–337, Feb. 2007.

[7] W. Lin, C. A. Wang, H. L. Le, B. Long, and Y. Huang, "Special assembly of laminated nanocomposite that mimics nacre," *Materials Science & Engineering C-Biomimetic and Supramolecular Systems*, vol. 28, no. 7, pp. 1031–1037, 2008.

[8] M. Sarikaya, "An Introduction to Biomimetics: A Structural Viewpoint," *Synthesis*, vol. 375, pp. 360–375, 1994.

[9] H. D. Espinosa, J. E. Rim, F. Barthelat, and M. J. Buehler, "Progress in Materials Science Merger of structure and material in nacre and bone – Perspectives on de novo biomimetic materials," *Progress in Materials Science*, vol. 54, no. May, pp. 1059–1100, 2009.

[10] M. A. Meyers, P. Y. Chen, A. Y. M. Lin, and Y. Seki, "Biological materials: Structure and mechanical properties," *Progress in Materials Science*, vol. 53, pp. 1–206, 2008.

[11] C. Knipprath, I. P. Bond, and R. S. Trask, "Biologically inspired crack delocalization in a high strain-rate environment.," *Journal of the Royal Society, Interface / the Royal Society*, vol. 9, no. 69, pp. 665–76, Apr. 2012.

[12] J. D. Currey, "Mechanical Properties of Mother of Pearl in Tension," *Proceedings of the Royal Society B: Biological Sciences*, vol. 196, no. 1125, pp. 443–463, Apr. 1977.

[13] P. Feraboli, E. Peitso, T. Cleveland, P. B. Stickler, and J. C. Halpin, "Notched behavior of prepreg-based discontinuous carbon fiber/epoxy systems," *Composites Part A: Applied Science and Manufacturing*, vol. 40, no. 3, pp. 289–299, Mar. 2009.

[14] K. He, R. Ganesan, and S. V. Hoa, "Interlaminar Stress and Delamination Analysis of Internally-Tapered Composite Laminates," *Journal of Reinforced Plastics and Composites*, vol. 23, no. 7, pp. 707–727, May 2004.

[15] M. R. Wisnom and M. Jones, "An Experimental and Analytical Study of Delamination of Unidirectional Specimens with Cut Central Plies," *Journal of Reinforced Plastics and Composites*, vol. 13, no. 8, pp. 722–739, Aug. 1994.

[16] Z. Petrossian and M. Wisnom, "Parametric study of delamination in composites with discontinuous plies using an analytical solution based on fracture mechanics," *Composites Part A: Applied Science and Manufacturing*, vol. 29, no. 4, pp. 403–414, 1998.

[17] M. I. Darby, J. M. Richards, and B. Yates, "Effect of discontinuous plies on the tensile strength of CFRP laminates," *Journal of Materials Science Letters*, vol. 4, no. 2, pp. 203–206, Feb. 1985.

[18] J. M. Richards, M. I. Darby, R. Baggott, G. H. Wosteim Holm, B. Yates, G. Dorey, and L. N. Phillips, "Effects of manufacturing defects on the mechanical properties of carbon fibre reinforced polyethersulphone laminates," *Journal of Materials Science*, vol. 24, no. 2, pp. 584–589, Feb. 1989.

[19] J. N. Baucom, J. P. Thomas, W. R. Pogue, and M. a. Siddiq Qidwai, “Tiled Composite Laminates,” *Journal of Composite Materials*, vol. 44, no. 26, pp. 3115–3132, Sep. 2010.

[20] I. Taketa, T. Okabe, and A. Kitano, “A new compression-molding approach using unidirectionally arrayed chopped strands,” *Composites Part A: Applied Science and Manufacturing*, vol. 39, no. 12, pp. 1884–1890, Dec. 2008.

[21] ASTM, “Standard Test Method for Flexural Properties of Unreinforced and Reinforced Plastics and Electrical Insulating Materials by Four-Point Bending 1,” *Annual Book of ASTM Standards*, vol. 02, no. Reapproved 2008, 2009.

[22] W. Cui, M. Wisnom, and M. Jones, “Effect of step spacing on delamination of tapered laminates,” *Composites Science and Technology*, vol. 52, no. 1, pp. 39–46, 1994.

[23] M. R. Wisnom and M. Jones, “Delamination of unidirectional glass fibre-epoxy with cut plies loaded in four point bending,” *Journal of Reinforced Plastics and Composites*, vol. 14, no. 1, pp. 45–59, 1995.

Figures

Figure 1

Figure 2

Figure 3

Figure 4

Figure 5

Figure 6

Figure 7

Figure 8

Figure 9

Figure 10

Figure 11

Figure 12

Figure 13

Figure 14

Figure 15

Figure 16

Tables

Table 1

Table 2

Table 3

Figure Captions

Figure 1 - The multiscale structure of nacre: (a) inside view of shell; (b) cross-section of a red abalone shell; (c) schematic of brick wall like microstructure; (d) optical micrograph showing tiling of tablets; (e) SEM of fracture surface. (Adapted from [9].)

Figure 2 - Ply terminations (a) butted ply ends (b) single ply drop (c) feature in butted joint.

Figure 3 - Vacuum assisted positioning guide allowing neighbouring plies to be positioned accurately before irreversible contact of the adhesive plies. (a) Exploded schematic view showing components of the guide. The base holds the bottom plies while the top section holds the top plies via vacuum. The plies on the top section are positioned, the backing material removed and then consolidated with the plies blow. (b) Three plies on the top section held in position by vacuum. (c) The top section (without plies or vacuum hose) and the base section with the consolidated plies.

Figure 4 - Micrograph of surface and internal ply cuts of a) 0.2mm, b) 0.5mm, c) 2.0mm and d) 3.0mm ply cut spacing in unloaded laminates. Each micrograph shows two double stack height resin pockets, one at a surface and one embedded within the central region.

Figure 5 - Beam dimensions of tested designs. Side and plan views (showing design C). Sections (equal to minor span of 75mm) of each design A-E shown with locations of ply cuts. Not to scale.

Figure 6 - Representative examples of load displacement curves for designs A, B and D (1.0mm ply cut spacing shown). The arrow indicates the resin pocket failure load in design B.

Figure 7 - Sequential failure (i-vii) of beam with a ply cut spacing >0.2mm at increasing cross head displacement. Delamination at C shown to propagate to the left of the sample, experimentally the delamination would propagate left or right. Delaminations shown in red. The illustrated failure was observed in-situ in real laminates, using of a macro-video camera.

Figure 8 - Prototype 1.0mm ply cut spacing specimen under flexural failure showing various delaminations. The LPDT has been removed from the experimental set-up for clarity.

Figure 9 - Representative load displacement curves for design C samples.

Figure 10 - Load displacement curves for all specimens of design E.

Figure 11 - Stills images of fracture progression in a prototype design E sample at increasing crosshead displacements (i-vi). LPDT removed for clarity. Scale bar: 50mm.

Figure 12 - Illustration of FEA model. Top: Beam and loading condition. Mid-left: Mesh refinement area around resin pocket. Mid-right: Mesh around roller-beam

contact. Bottom: Stress enquiry lines 25μm away from material boundary within mesh refinement area. 1mm ply cut spacing shown in illustration.

Figure 13 - σ_{11} stresses above resin pockets of various sizes.

Figure 14 - σ_{11} stresses below resin pockets of various sizes.

Figure 15 - σ_{11} stress distributions for different ply cut spacings. Scale bar in MPa.

Figure 16 - Peak σ_{11} stresses above resin pocket as a function of total model element number.

Figure(s)

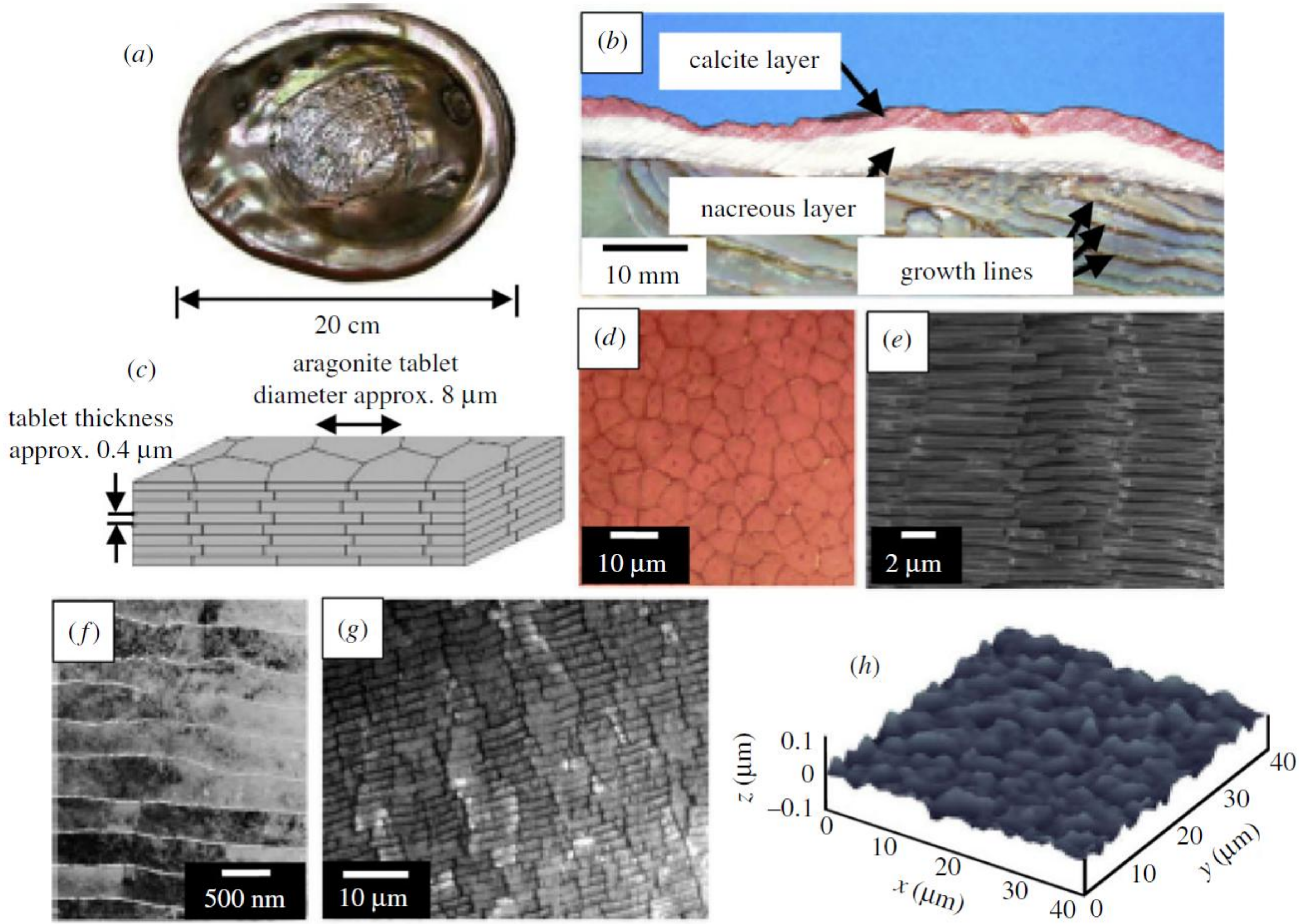

(a)
20 cm
(b)
calcite layer
nacreous layer
10 mm
growth lines
(c)
aragonite tablet
diameter approx. 8 μm
tablet thickness
approx. 0.4 μm
(d)
10 μm
(e)
2 μm
(f)
500 nm
(g)
10 μm
(h)
z (μm)
0.1
0
−0.1
0
10
20
30
40
x (μm)
0
10
20
30
40
y (μm)

Figure(s)

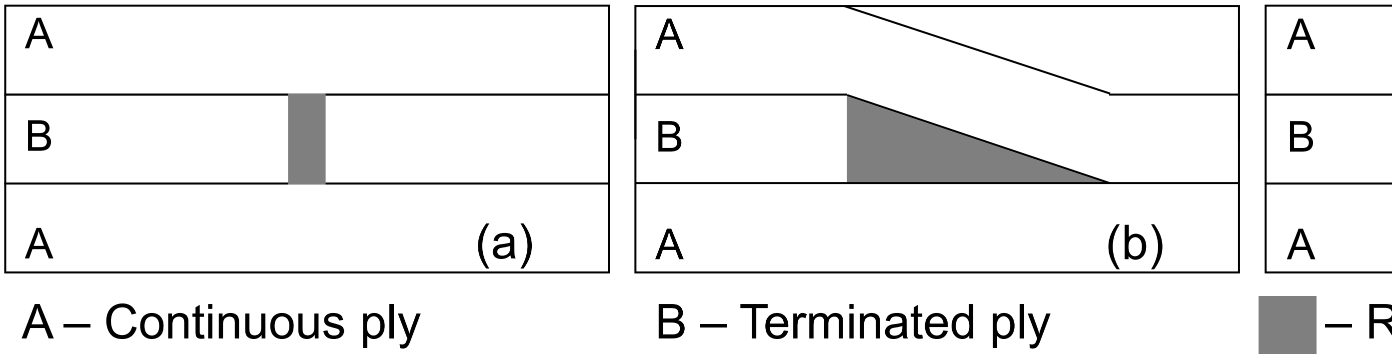
A
B
A
(a)
A
B
A
(b)
A
B
A
(c)
A – Continuous ply
B – Terminated ply
– Resin pocket

Figure(s)

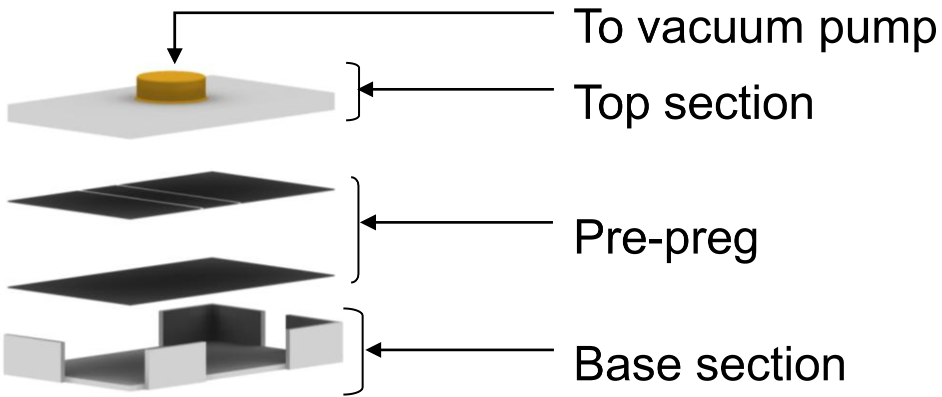

(a)

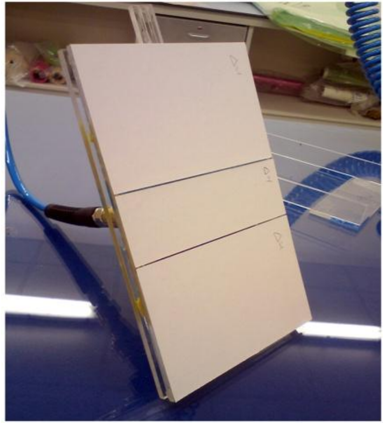

(b)

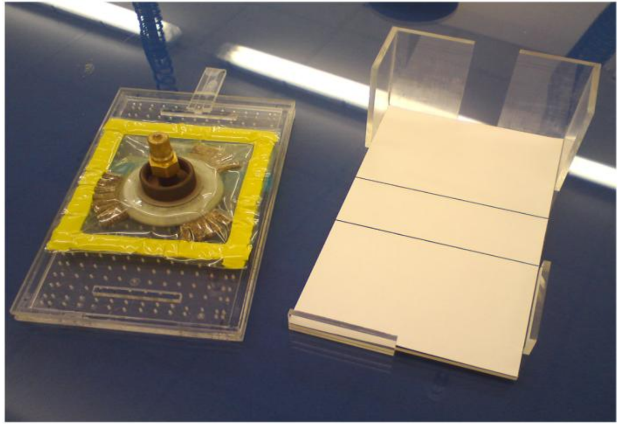

(c)

Figure(s)

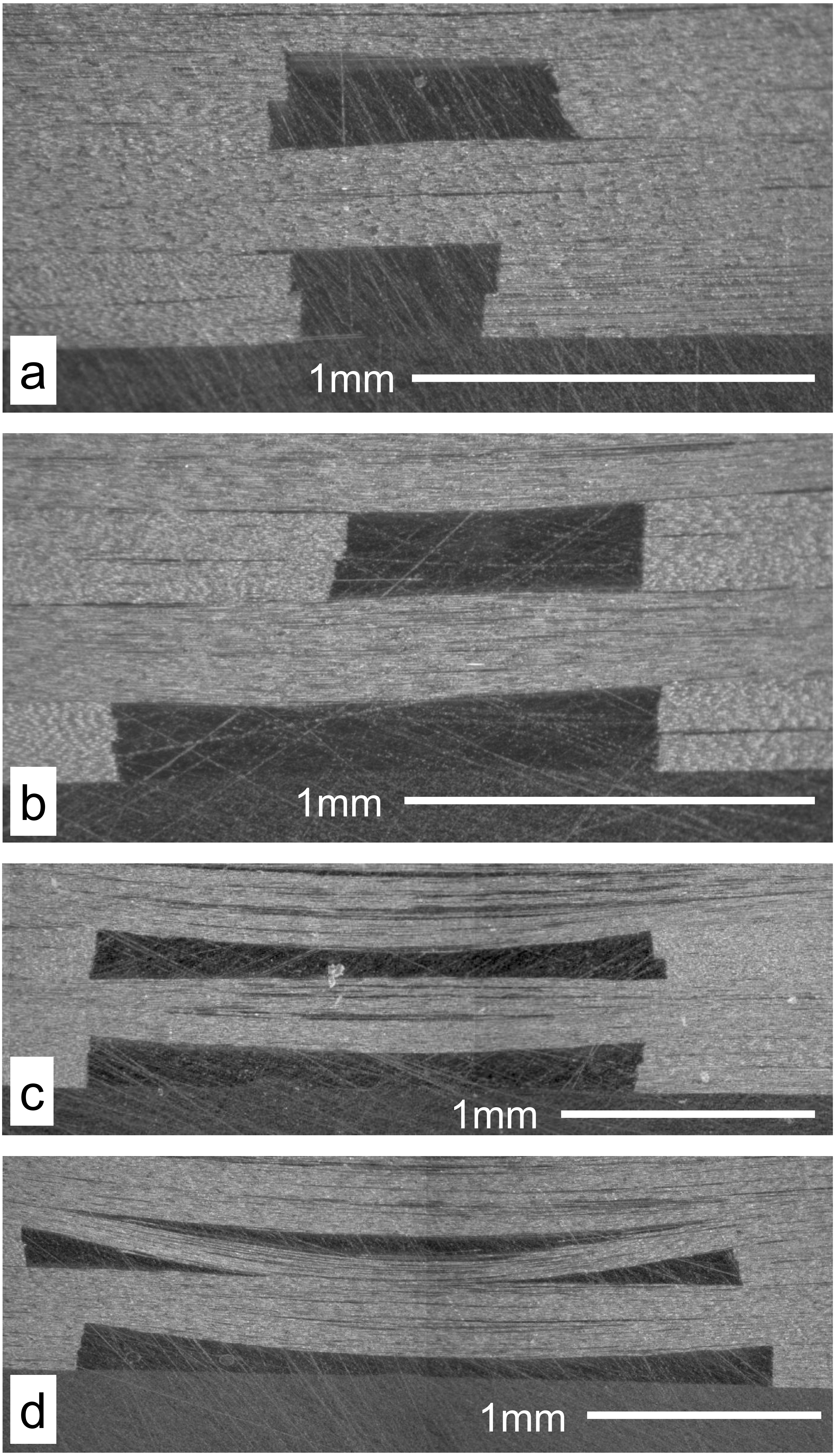

Figure(s)

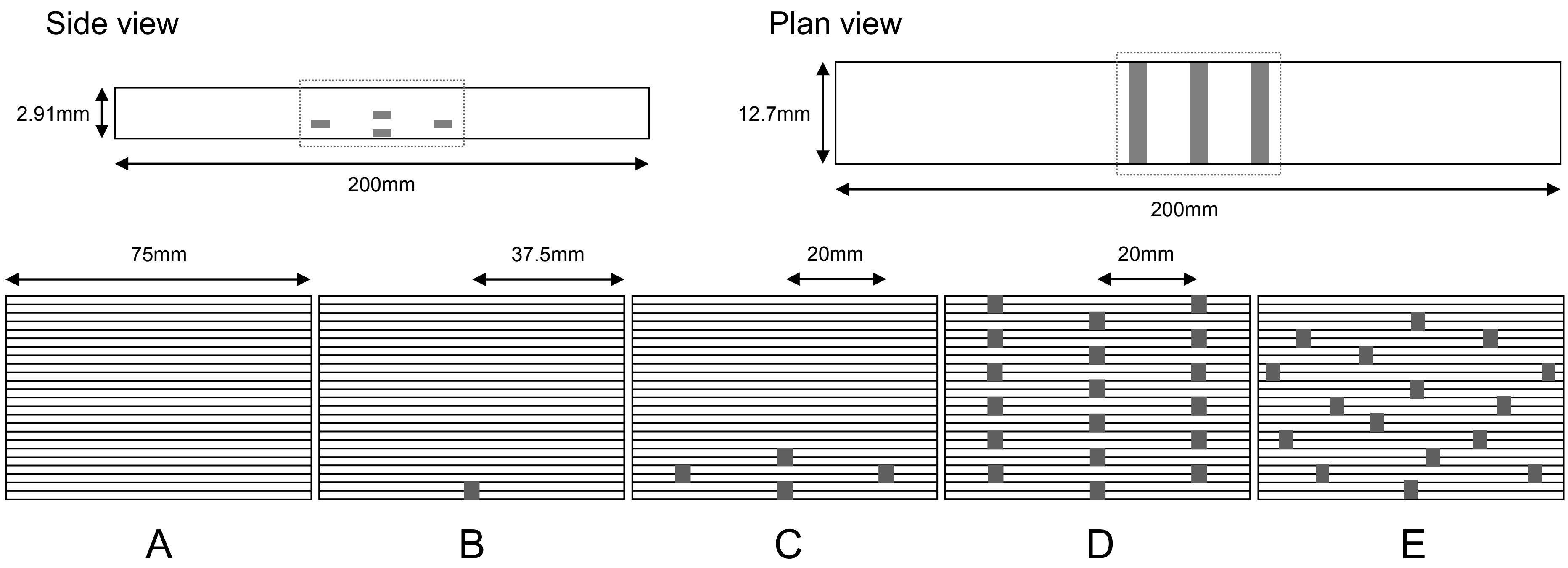

Side view
2.91mm
200mm
Plan view
12.7mm
200mm
75mm
37.5mm
20mm
20mm
A
B
C
D
E

Figure(s)

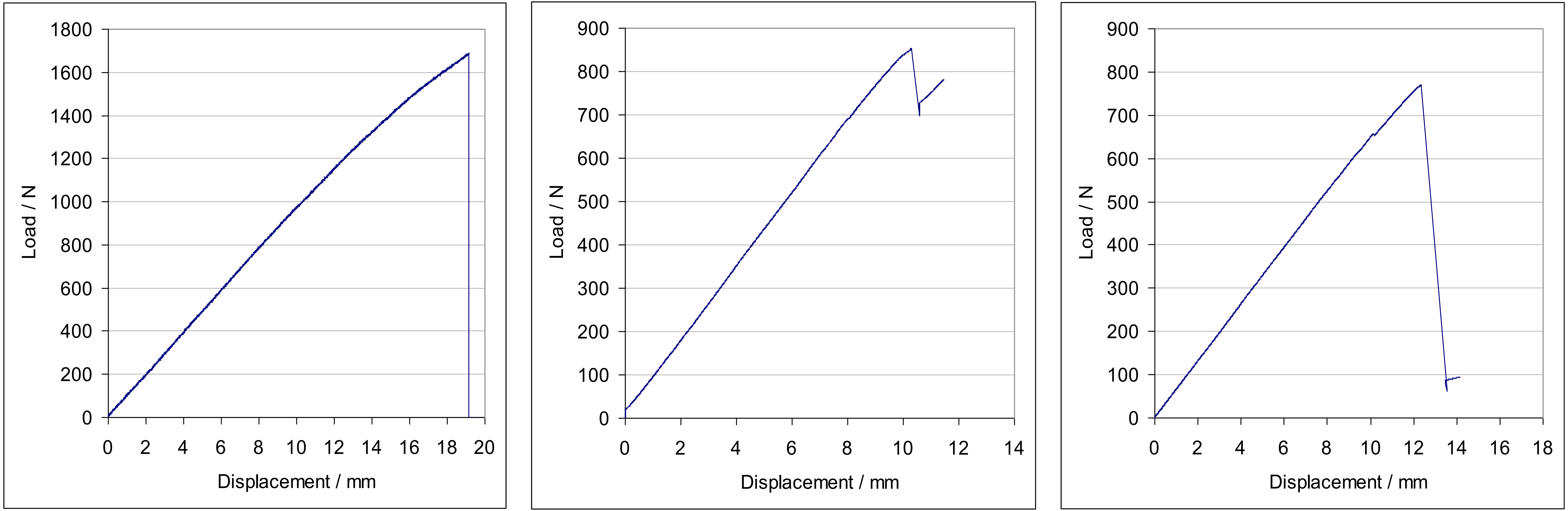

Design A Design B Design D

Figure(s)

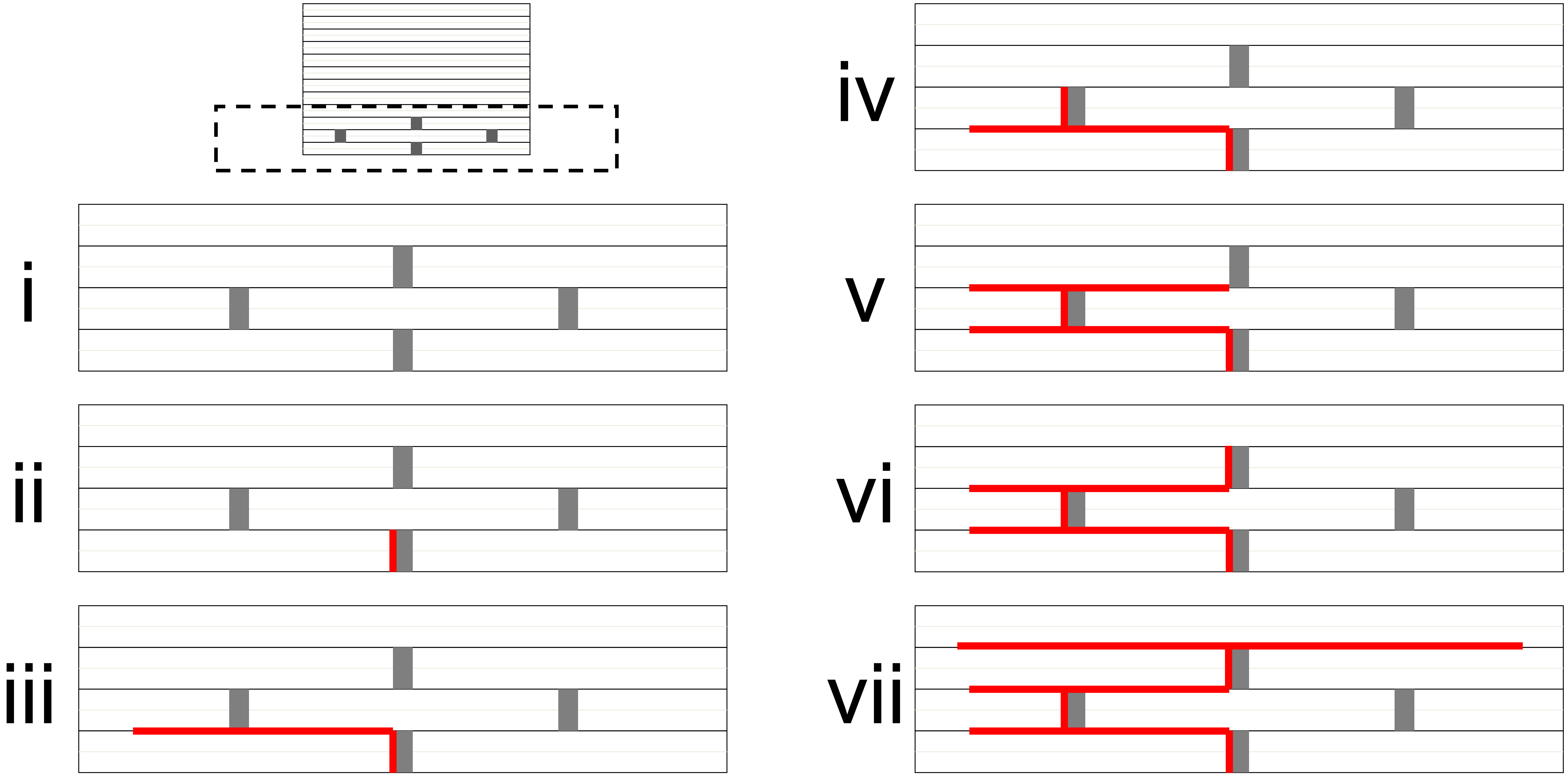

Figure(s)

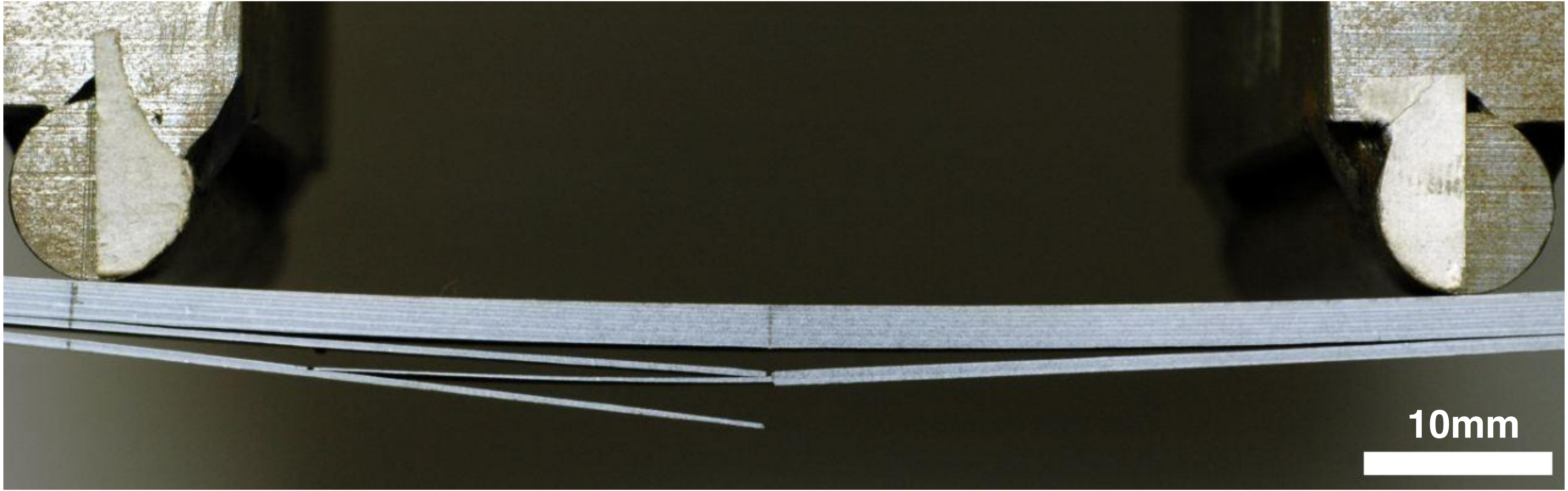

Figure(s)

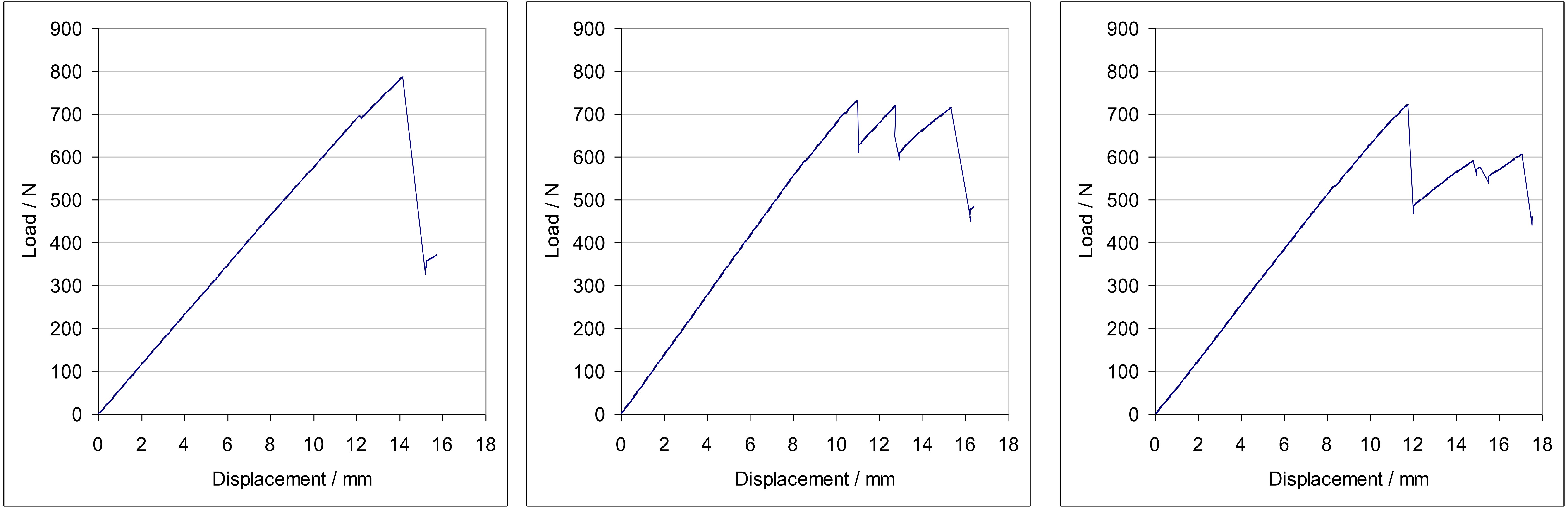

0.2mm 1.0mm 2.0mm

Figure(s)

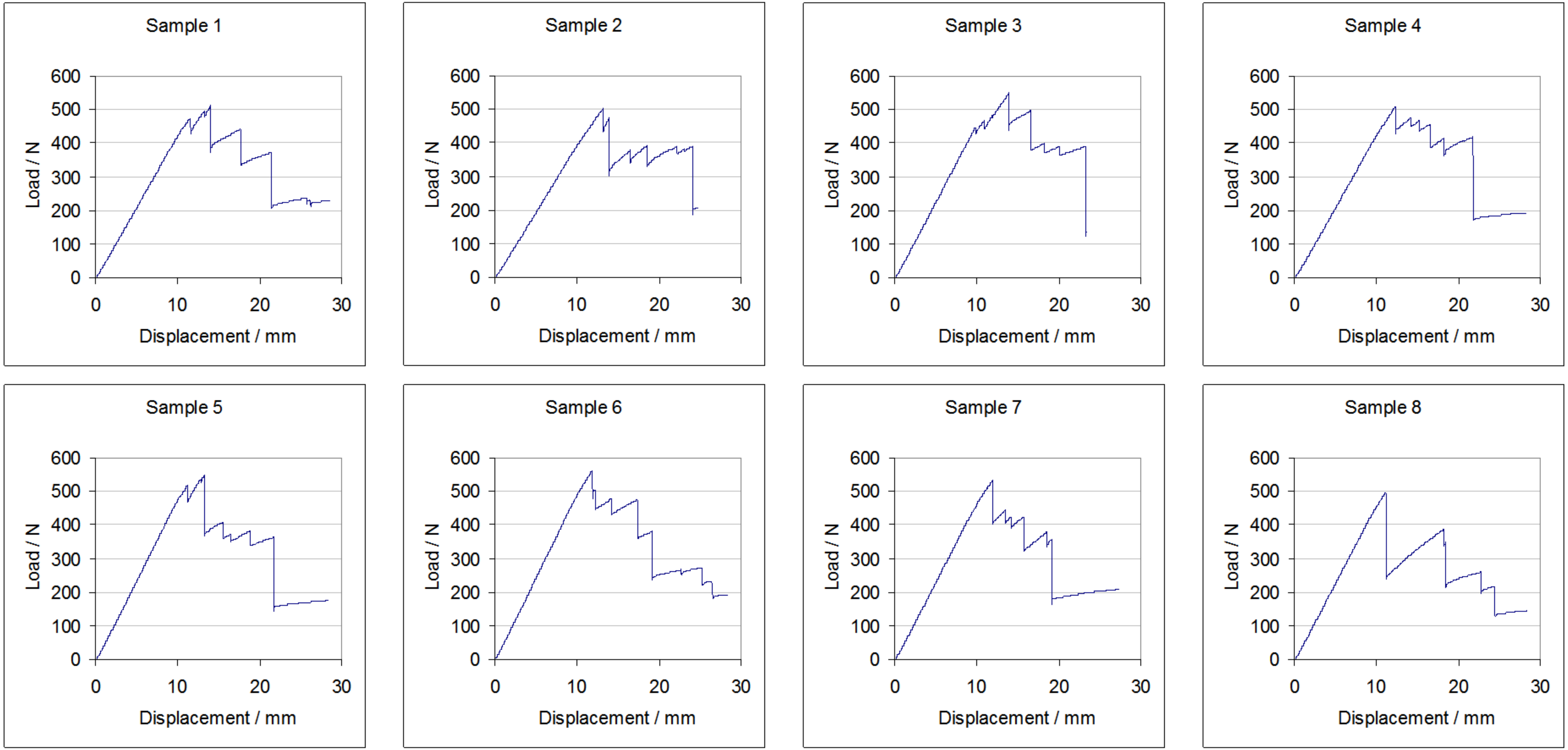
Sample 1
Sample 2
Sample 3
Sample 4
Sample 5
Sample 6
Sample 7
Sample 8
Load / N
Displacement / mm
0
100
200
300
400
500
600
0
10
20
30

Figure(s)

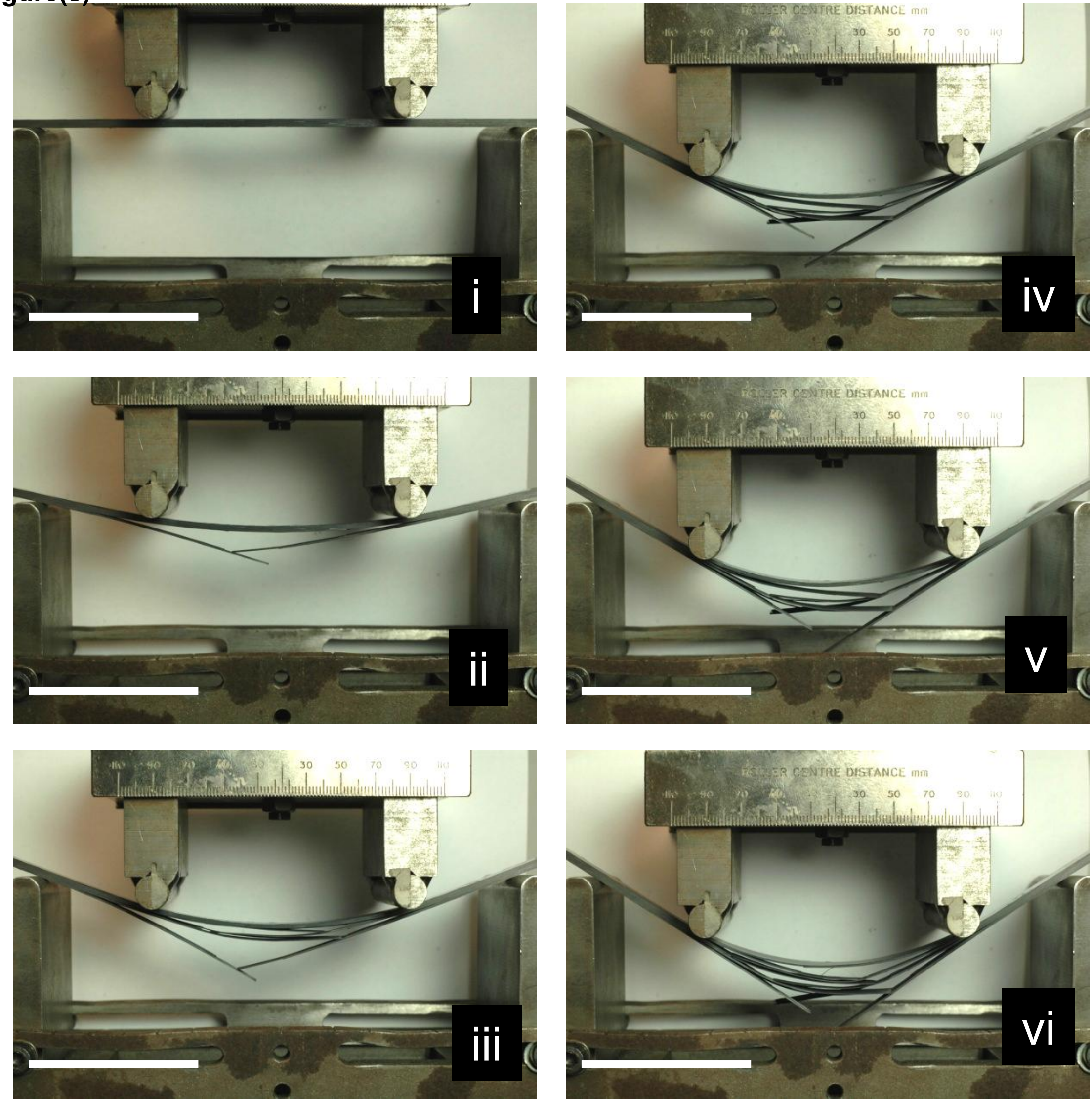

Figure(s)

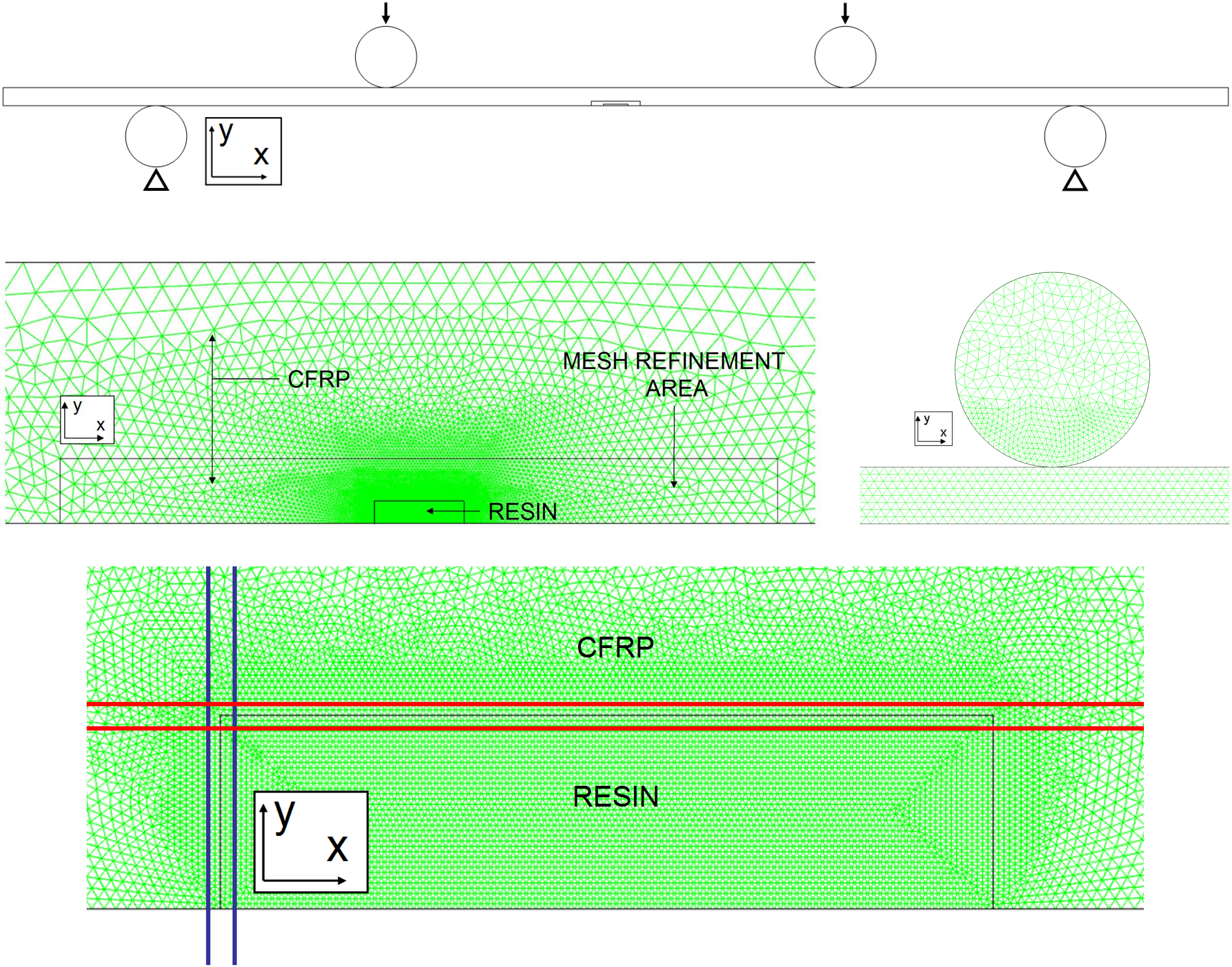

Figure(s)

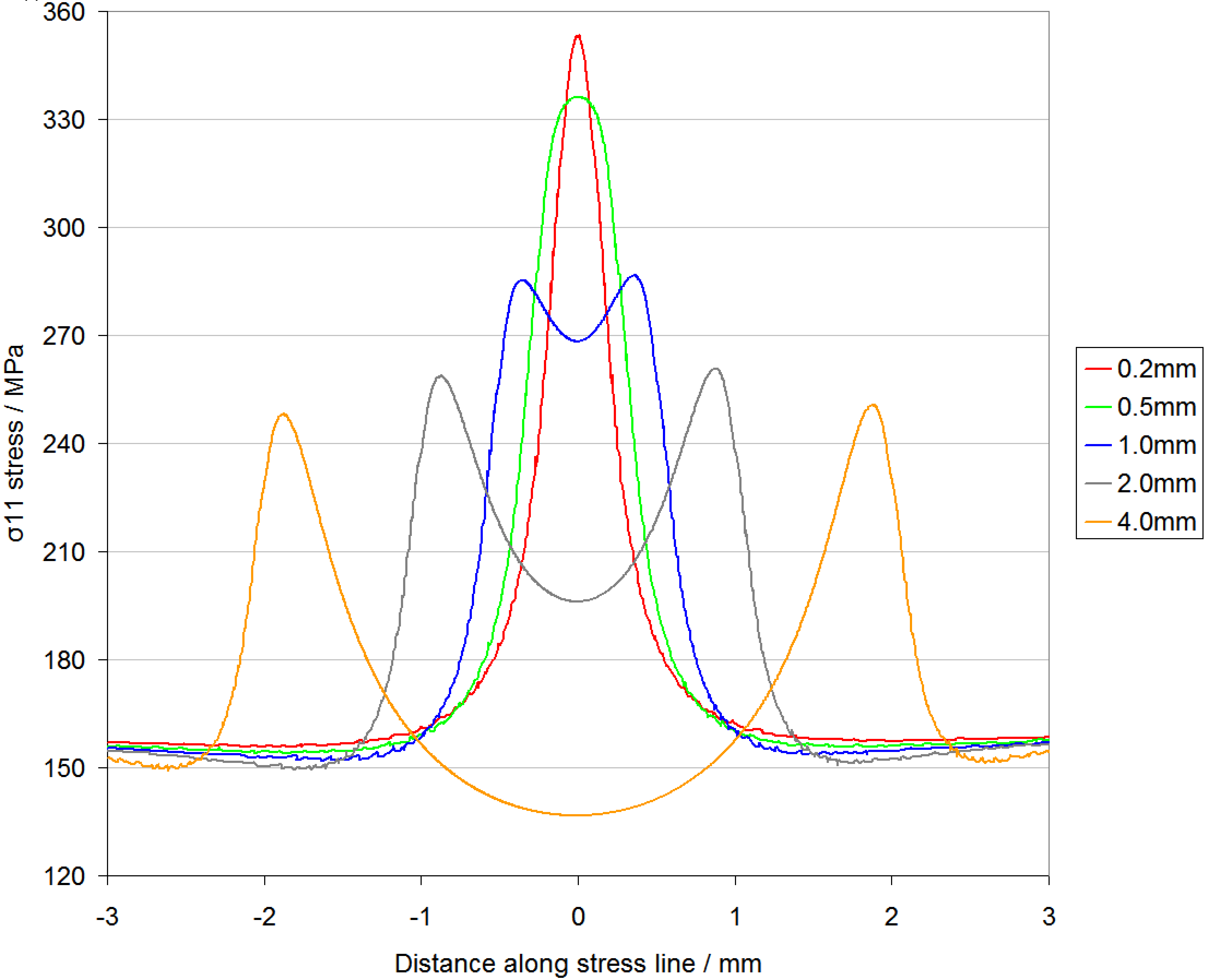

σ11 stress / MPa
360
330
300
270
240
210
180
150
120
-3
-2
-1
0
1
2
3
Distance along stress line / mm
0.2mm
0.5mm
1.0mm
2.0mm
4.0mm

Figure(s)

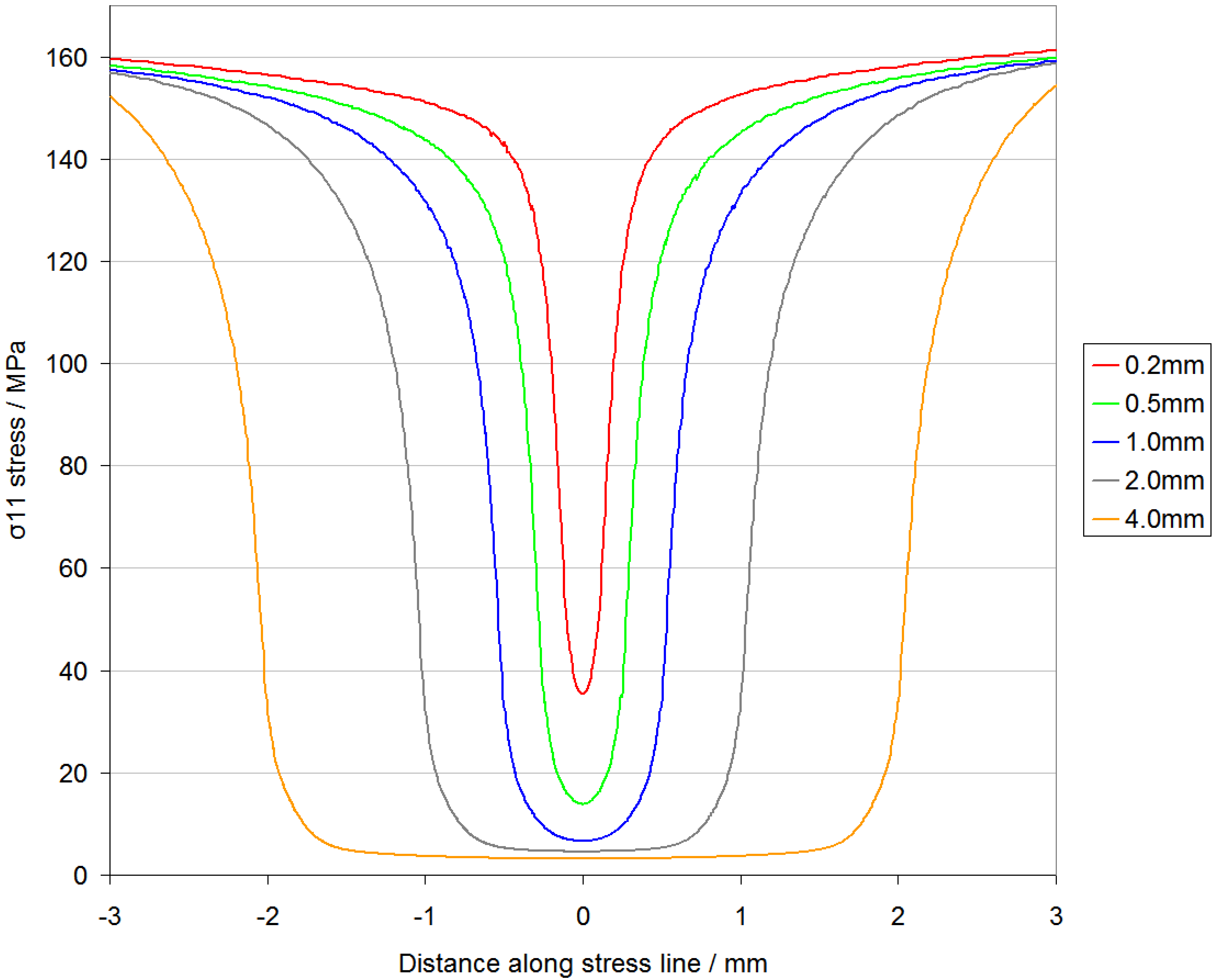

160
140
120
100
80
60
40
20
0
σ11 stress / MPa
-3
-2
-1
0
1
2
3
Distance along stress line / mm
0.2mm
0.5mm
1.0mm
2.0mm
4.0mm

Figure(s)

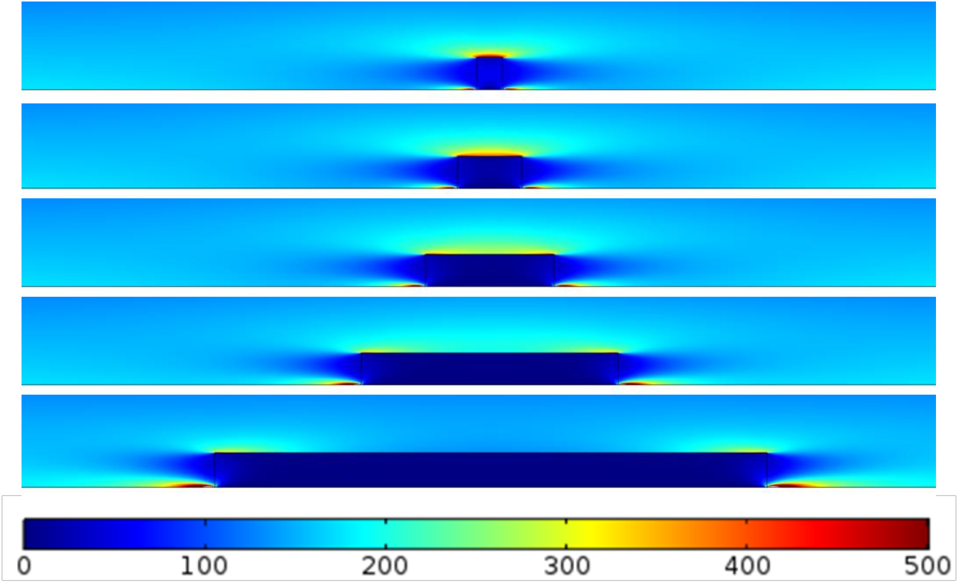

Figure(s)

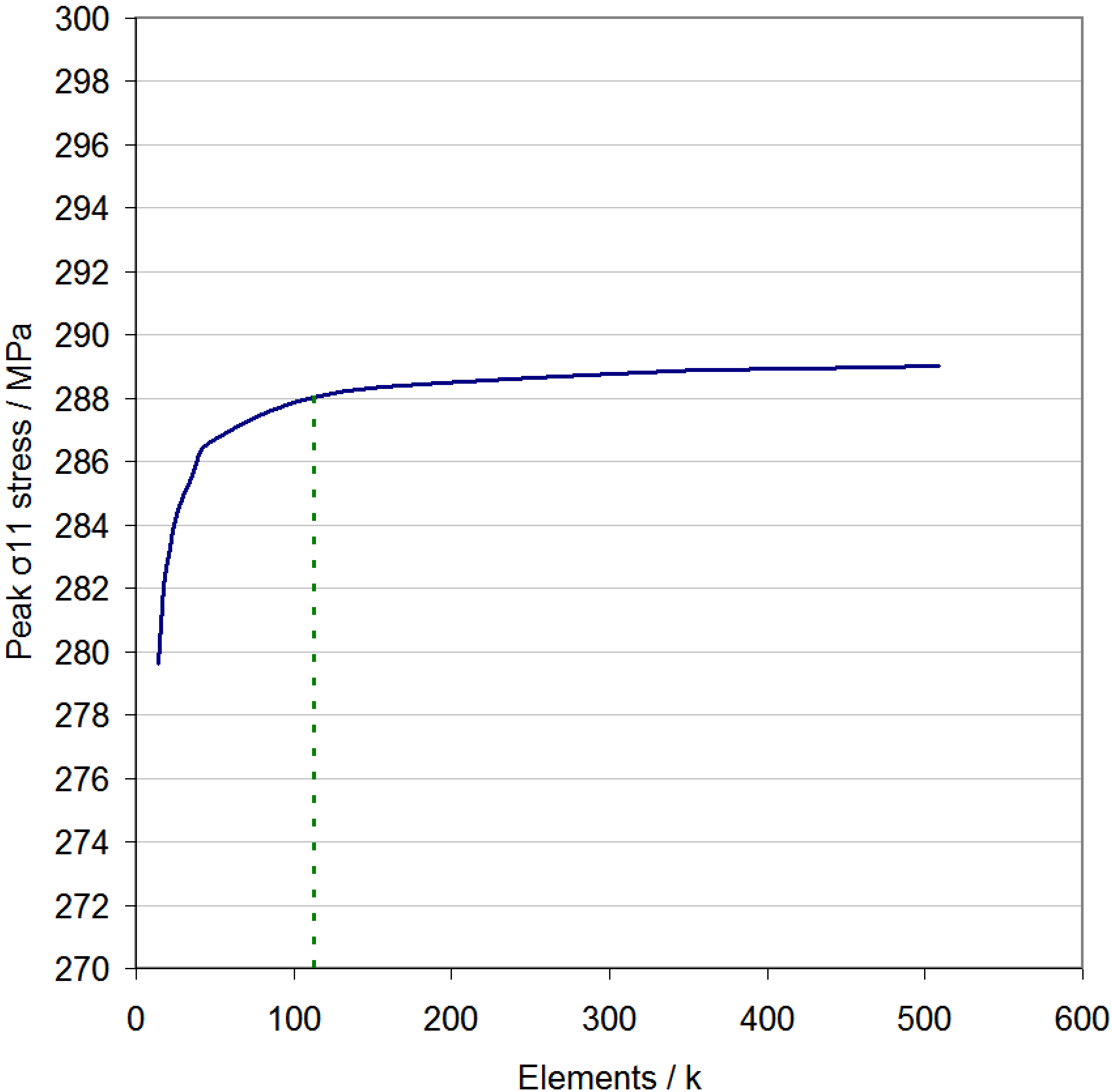

300
298
296
294
292
290
288
286
284
282
280
278
276
274
272
270
Peak σ11 stress / MPa
0
100
200
300
400
500
600
Elements / k

Table(s)

Tables

Table 1 – Flexural strengths of designs A-E as calculated at the first observable delamination/fracture. Standard deviations given in parentheses.

Design	Ply cut spacing / mm			
	UD	0.2	1.0	2.0
A	1427 (151) MPa	-	-	-
B	-	921 (71) MPa	781 (65) MPa	802 (69) MPa
C	-	829 (100) MPa	821 (61) MPa	797 (79) MPa
D	-	750 (36) MPa	756 (27) MPa	745 (15) MPa
E	-	-	672 (28) MPa	-

Table 2 - Single resin pocket fracture loads. Standard deviations given in parentheses.

Failure Event	Ply cut spacing / mm		
	0.2	1.0	2.0
Resin pocket failure / N	434 (106)	688 (53)	711 (77)
Delamination onset / N	908 (62)	862 (65)	883 (81)
Strength / MPa	921 (71)	781 (65)	802 (69)

Table 3 - Material properties used for FEA.

Material property	Composite	Resin Pocket	Rollers
Cured ply thickness / mm	0.13	-	-
Number of plies	24	-	-
E_{11} / GPa	163.00	4.67	200.00
$E_{22}=E_{33}$ / GPa	10.00	-	-
$G_{12}= G_{13}$ / GPa	4.8	-	-
G_{23} / GPa	3.2	-	-
$V_{12}= V_{13}$	0.31	0.35	0.30
V_{32}	0.52	-	-